Design methodology for dual-band hybrid antennas with off-resonance loading

Naeem, U., Bila, S., Thévenot, M., & Arnaud, E. (2017). Design methodology for dual-band hybrid antennas with off-resonance loading. *IET Microwaves, Antennas and Propagation*, *11*(14), 2077-2082. https://doi.org/10.1049/iet-map.2017.0163

Published in:
IET Microwaves, Antennas and Propagation

Document Version:
Peer reviewed version

Queen's University Belfast - Research Portal:
Link to publication record in Queen's University Belfast Research Portal

Publisher rights
© 2017.The Institution of Engineering and Technology. This work is made available online in accordance with the publisher's policies. Please refer to any applicable terms of use of the publisher.

General rights
Copyright for the publications made accessible via the Queen's University Belfast Research Portal is retained by the author(s) and / or other copyright owners and it is a condition of accessing these publications that users recognise and abide by the legal requirements associated with these rights.

Take down policy
The Research Portal is Queen's institutional repository that provides access to Queen's research output. Every effort has been made to ensure that content in the Research Portal does not infringe any person's rights, or applicable UK laws. If you discover content in the Research Portal that you believe breaches copyright or violates any law, please contact openaccess@qub.ac.uk.

Download date:05. May. 2023

"This paper is a postprint of a paper submitted to and accepted for publication in IET Microwaves, Antennas and Propagation and is subject to Institution of Engineering and Technology Copyright. The copy of record is available at the IET Digital Library"

Design Methodology for Dual-Band Hybrid Antennas with Off-Resonance Loading

Umair Naeem [1*], Stéphane Bila [2], Marc Thévenot [2], and Eric Arnaud [2]

[1] ECIT Institute, Queen's University of Belfast, NI Science Park, Queen's Road, Queen's Island, Belfast, BT3 9DT, UK
[2] XLIM UMR 7252, Université de Limoges/CNRS, 123 Avenue Albert Thomas, 87060 Limoges, France
*umairnm@hotmail.com

Abstract: The presented work proposes a generalized design methodology for dual-band hybrid antennas. The methodology is applied to a dual-band hybrid antenna system operating in two modes; one allows the antenna to radiate at a lower frequency band, whereas the other operates the antenna at a higher frequency band. The lower band radiating element is also responsible for exciting the higher band radiating element. Since the two radiating modes depend on each other, the antenna system is characterized in detail to achieve efficient impedance matching for both the modes. An efficient model is proposed that models the true behaviour of the system. A hybrid dual-band antenna has been modelled, designed and fabricated. Test results exhibit desired radiation behaviour as well as good impedance match for both the bands. The proposed design methodology allows the design of antenna for each radiating mode quasi-independently. This design methodology can be applied to any similar type of antenna which exploits multiple radiating elements where one is loaded by another.

1. Introduction

With the exponential growth in advanced telecommunication services, there is an ever increasing demand for systems and components supporting multiple standards while being as compact as possible. Embedding multiple functionalities in a single package leads to the concept of system-on-package (SOP). Several designs can be found in literature that propose systems with integrated antenna and front-ends on the same package [1-3].

For designing compact multi-standard systems, front-end antennas remain the most challenging part of any system. Several research works propose multi-functional and reconfigurable antennas [4-6]. In [7-9] different modes are exploited to realize multiple-polarized antennas. Multiple frequency bands can also be achieved by exploiting multiple modes of the same radiating element [10-14]. Although multiple bands can be radiated using same antenna, but there is always a compromise in the radiation efficiency of the antenna system. Multi-band antennas can also be realized through hybrid structures [15-17] with each type of radiating element supporting different frequency band. In order to address the higher data rate requirements, front-ends with large bandwidths are desired. Monopoles, diploes and Planar inverted-F antennas are used extensively as a solution to this problem. A dipole loaded with dielectric was presented in [18] to achieve wide bandwidth. The integration of such type of structures with the modern high density electronics is a major bottleneck for achieving compact and large bandwidth systems. On the other hand the dielectric resonator antennas (DRAs) offer superior radiation efficiency, higher gain and more compactness that can be used to realize antenna front-ends for high performance systems. In [19] a bulky 3D structure of dielectric loaded monopole antenna was presented. It was focused on the ultra-wideband (UWB) operation of the antenna (i.e. 1-20 GHz) which requires different design approach than the design of narrow band resonant structures. Furthermore, no account of interaction among the different radiation modes was presented in [19].

The presented work thoroughly discusses the design procedure of the dual-band antenna, as well as its coupling and radiation characteristics. The dual-band antenna is formed by combining the broadband monopole and more efficient DRA. A reliable circuit model will be proposed which can be used for co-designing of filter-antenna system as proposed in [20]. The designed antenna system can be used for Wi-Fi applications (IEEE 802.11(a) and 802.11(b)) as shown in [21] in which design concept of a filter-antenna front-end was shown. In this proposed work $TE_{01\delta}$ mode is excited, and will be validated through radiation characteristics of the fabricated antenna. To the authors' knowledge no significant work has been found in literature that proposes design methodology for such hybrid antennas.

2. Hybrid DRA-Monopole Antenna

The initial dimensions of the antenna structure are computed from the design equations well known in the literature. At first the individual radiating elements are characterized so that models generated can be used for the combined inter-dependent antenna system. The antenna system under discussion consists of two modes, namely the DRA mode, and the monopole antenna mode. The DRA mode will provide the radiation for the upper frequency band centred at f_U = 5.5 GHz. The monopole antenna mode will radiate at a lower frequency band which is centred at f_L = 2.45 GHz. A split-cylindrical DRA radiating in $TE_{01\delta}$ mode is coupled to a monopole antenna to achieve a dual-

band response. The DRA requires a strong coupling with the monopole antenna, while maintaining the required performance of the overall antenna system. In order to achieve optimal coupling of the DRA mode, an efficient monopole antenna structure is proposed which is optimized for both the modes.

2.1. The DRA Mode

A split-cylindrical—a cylinder cut into half by a plane along its rotational axis—dielectric resonator antenna is chosen for the DRA mode radiation. This structure supports the desired $TE_{01\delta}$ mode. For the DRA mode this particular structure and mode is selected due to its ability to efficiently couple to the monopole antenna. Consider a split-cylindrical shape dielectric resonator antenna of diameter d and height h, as shown in Fig. 1(a). The resonator is placed on an infinite ground plane. The field distribution, for $TE_{01\delta}$ mode, inside the dielectric resonator is shown in Figs. 1(b) and (c). The material and dimensions of the dielectric resonator are chosen so as to achieve the required impedance bandwidth. The impedance bandwidth is a function of material's relative permittivity ε_r and the aspect ratio (diameter 'd' to height 'h' ratio) [22]. Choosing a dielectric material, made of Alumina (tan δ= 0.002), of relative permittivity ε_r = 9.5, d = 18mm and h = 6mm, the DRA will yield an impedance bandwidth of >10%.

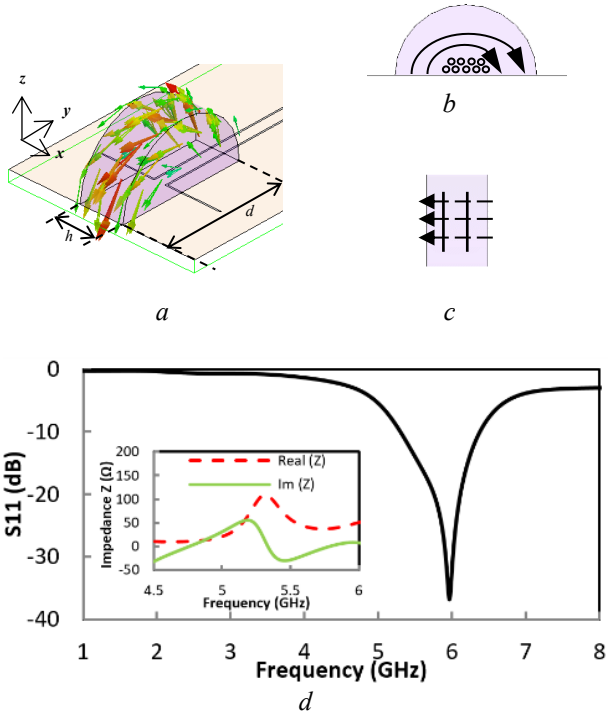

Fig. 1. *Sketch of E fields (solid line) and H fields (dashed lines), for $TE_{01\delta}$ mode, inside the dielectric structure*
(a) Split-cylindrical DRA on infinite ground plane, **(b)** y-z plane, **(c)** x-z plane, **(d)** Wideband return loss of the antenna.

The resonant frequency of the DR can be found from [23]. For a full cylindrical DR the resonant frequency is found to be 5.79 GHz. In order to investigate the radiation and impedance characteristics of the $TE_{01\delta}$ mode the structure shown in Fig. 1(a) is simulated. It can be observed from Fig. 1 that the desired mode is efficiently excited in the DR.

2.2. The Monopole Antenna Mode

Radiation in the lower frequency band is realized through a folded monopole antenna structure which is excited through a grounded coplanar waveguide feed, as shown in Fig. 2. The antenna is matched through a quarter wave transformer. For this structure the substrate is chosen to be Rogers RT5880 having ε_r = 2.2 and height of the substrate is 1.575mm. The length of the monopole can be approximated as $l_1 + l_2 = \lambda_g/4$ (Fig. 2). The ground plane of the monopole antenna influences the gain, impedance and the resonant frequency, therefore it must be large enough and the open end of the monopole must be sufficiently spaced from the ground. Fig. 2 shows good impedance matching of the folded monopole antenna configuration.

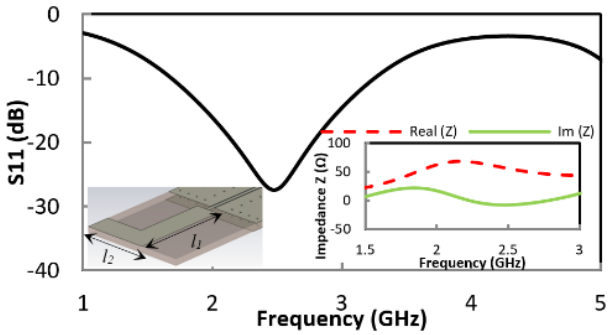

Fig. 2. *Return loss of the monopole antenna. Structure for monopole antenna mode (bottom left inset). Input impedance of the antenna (bottom right inset).*

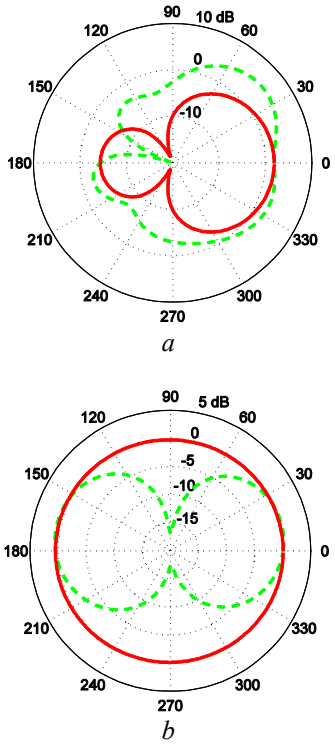

Fig. 3. *Radiation patterns (Gain vs θ). ϕ= 0° (x-z plane) in solid red, and ϕ = 90° (y-z plane) in dashed green*
(a) DRA mode, **(b)** Monopole mode

The radiation patterns of the simulated antenna structures are illustrated in Fig. 3. These patterns will be used as a reference and will be compared with the radiation patterns of the final structure.

2.3. Combined Antenna System

The two antenna systems (DRA and the monopole antenna) are investigated separately, both are designed in such a manner so that they are compatible with each other. The dielectric resonator is now placed, as shown in Fig. 4(a) and (b), on the designed monopole structure to achieve a dual-band antenna.

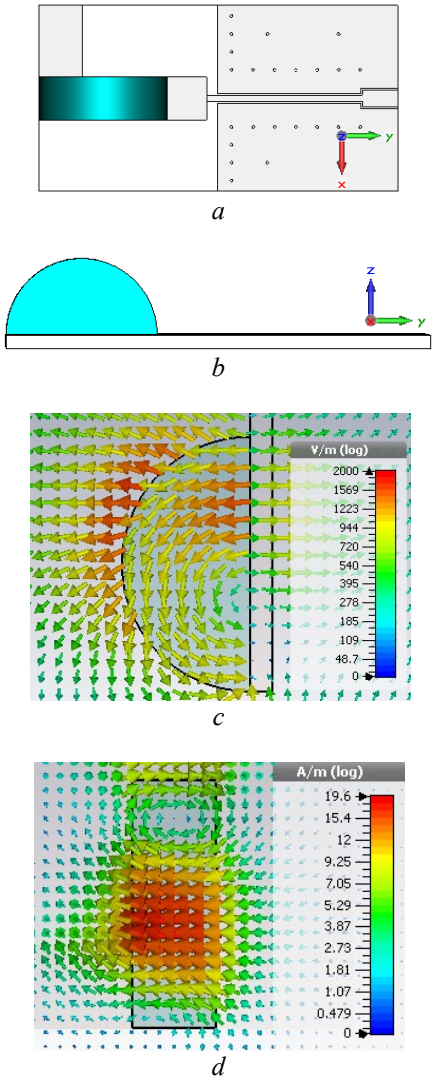

Fig. 4. *Combined DRA-Monopole antenna system.* **(a)** Top View, **(b)** Side View, **(c)** Plot of E fields for $TE_{01\delta}$ mode, inside the dielectric structure, **(d)** Plot of H fields $TE_{01\delta}$ mode, inside the dielectric structure. The fields are shown at the cut-planes passing through the dielectric resonator.

Observing the E and H fields inside the dielectric resonator (Fig. 4(c) and (d)), it can be verified that the $TE_{01\delta}$ mode is excited in the DR at high frequency (DRA mode).

It can be observed from Fig. 5 that when the shape of the dielectric material is changed the DR mode is changed significantly whereas there is negligible change in the monopole mode.

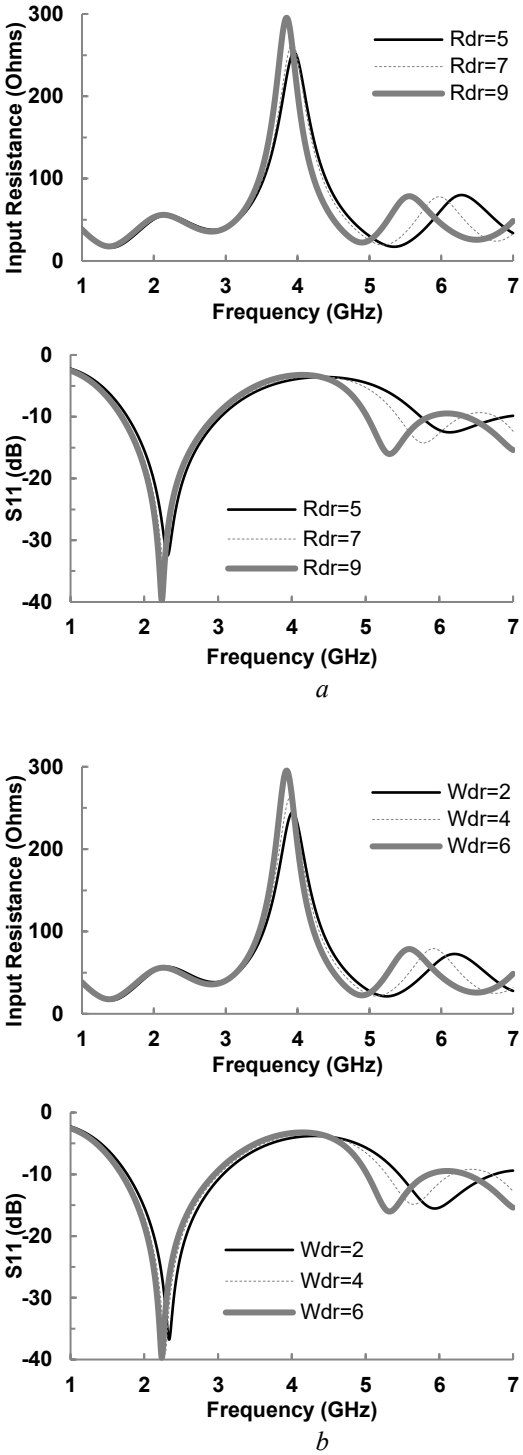

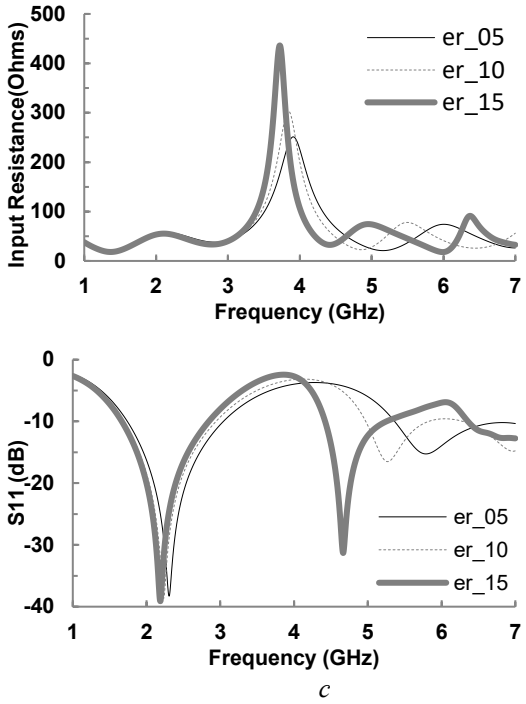

c

Fig. 5. *The antenna's input property when,*
(a) the radius, R_{dr}, of dielectric material is changed, **(b)** the width, W_{dr}, of dielectric material is changed, **(c)** the relative permittivity of dielectric material is changed

It is evident from Fig. 5(c) that the change in relative permittivity allows the change in DRA mode without effecting much to the monopole mode.

The proposed antenna structure exhibits dual radiating modes that can be designed independently, where one mode provides the coupling mechanism for the other without much affecting on its radiation characteristics.

3. Coupling Characteristics

In order to properly model the whole antenna system, first individual antenna elements are characterized by simulating their input impedances for similar feeding structures as detailed in the previous section. The element values extracted for a particular resonating mode will remain same for the combined model this can be verified from the full-wave simulation of the combined structure. This section will detail the coupling characteristics as a function of position of DR on the monopole which will depend on the surface current distribution on the monopole, which eventually leads to the extraction of coupling coefficients. The monopole antenna, coupled to the source through quarter wave impedance transformer, shown in Fig. 2 can be modelled as a parallel resonant circuit as illustrated in Fig. 6(a). For parallel resonant circuit, loaded quality factor Q_m for monopole mode is given by:

$$Q_m = \frac{R_{Tm}}{\omega_o L} = \frac{f_o}{f^{-90} - f^{+90}} \quad \text{(1-a)}$$

$$N_{sm}{}^2 = \left(\frac{1}{R_{Tm}} - \frac{1}{R_m}\right) Z \quad \text{(1-b)}$$

R_{Tm} is the equivalent resistance of parallel RLC coupled to source. f_o is the resonant frequency and $f_{+/-90}$ are the frequencies at which phase of S_{11} is 90° above and below f_o (from filter theory). The extracted circuit model values are: N_{sm} = 1.6, R_m = 27 Ω, L_m = 1 nH, C_m = 5.44 pF.

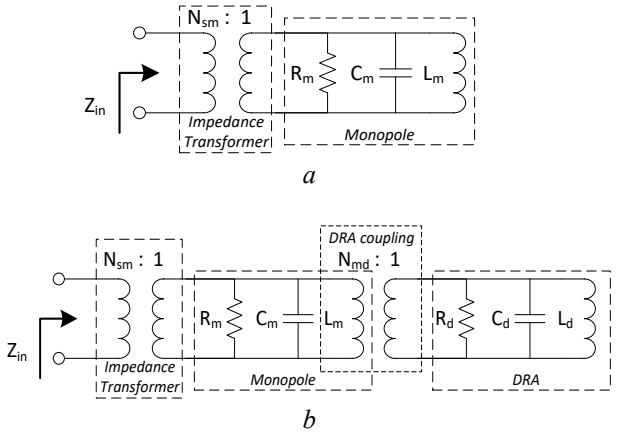

Fig. 6. *Circuit model*
(a) Monopole antenna, **(b)** DRA coupled to the monopole antenna

Consider the circuit model of DRA coupled to the monopole antenna as shown in Fig. 6(b). The monopole antenna is coupled to the source with an impedance transformer, whereas the DRA is coupled to the source through monopole and the transformer. Since the DRA operates at a higher frequency than the monopole it merely exhibits a loading effect on the monopole antenna mode. The monopole acts as an efficient coupling element for the DRA mode.

$$Q_d = \frac{R_{Td}}{\omega_o L} \quad \text{(2-a)}$$

$$N_{md}{}^2 = \left(\frac{1}{R_{Td}} - \frac{1}{R_d}\right) R_{Tm} \quad \text{(2-b)}$$

Similarly for DRA mode loaded quality factor is Q_d and R_{Td} is the equivalent resistance of parallel RLC as defined by (2). The coupling N_{sm} is realized through a quarter wave transformer. The coupling N_{md} is a function of the position of DR on monopole antenna. The coupling N_{md} can carefully be optimized by studying the surface currents on the monopole, at both the frequency bands – centred at f_L and at f_U. It is evident that more the DR covers the monopole area, where electric fields are maximum, more predominate will be the loading effect on the monopole mode (at f_L). A structure is therefore proposed which caters for such an effect. Fig. 7, shows the surface current distribution on the monopole antenna at f_L. This structure is less sensitive to the effects of DR at f_L, as the DR does not cover the portion of maximum E field. As can be seen from Fig. 7 the maximum current is in the unfolded (along y-axis) branch, the radiation pattern is similar to the ideal monopole as illustrated in Fig. 3(b). As the DR is over the area of monopole where magnetic field is strong the DR is tightly coupled to the source at upper frequency band f_U. The DR is placed on the monopole antenna, as shown in Fig. 7(c), where the maximum coupling for the $TE_{01\delta}$ mode is achieved.

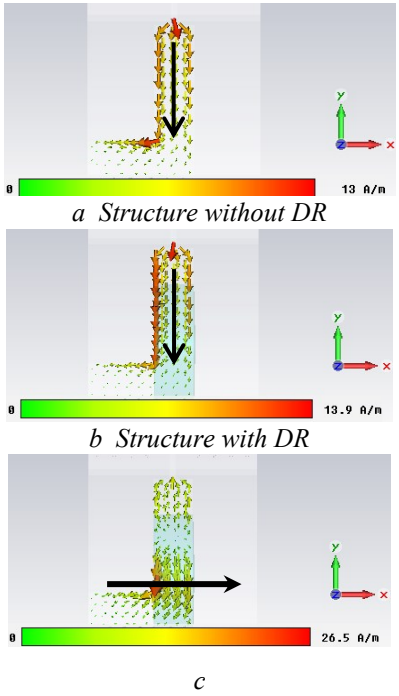

a Structure without DR

b Structure with DR

c

Fig. 7. *Surface current distribution*
(a) Surface current distribution on the structure without DR at 2.45 GHz, **(b)** Surface current distribution on the structure with DR at 2.45 GHz. The arrows show the equivalent short electric monopoles (for the monopole antenna mode), **(c)** Surface current distribution on the structure with DR at 5.5 GHz. The arrow shows the equivalent short magnetic dipole (for the $TE_{01\delta}$ DRA mode)

Consider three different configurations of the antenna system as shown in Figs. 8(a), (b) and (c) which differs by the placement of DR on the monopole antenna. The input impedances for the three configurations are detailed in Fig. 8(d), the extracted quality factors are shown in Fig. 9(a) and subsequent extracted element values for the proposed circuit model are given in Table 1, where R_m = 27 Ω, L_m = 1 nH, C_m = 5.44 pF.

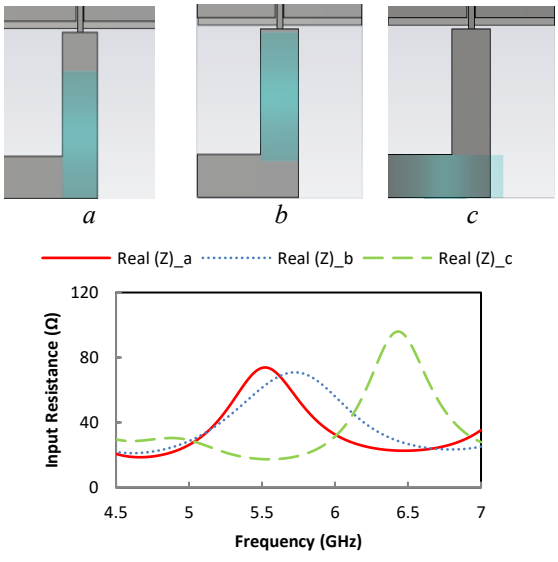

a *b* *c*

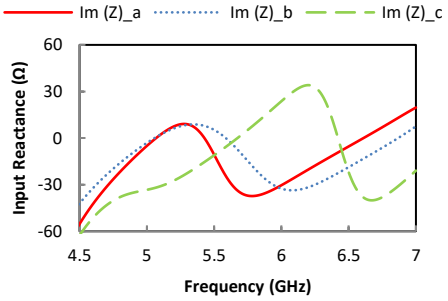

d

Fig. 8. *Input impedances for the three configurations*
(a) Configuration *a* of the antenna system, **(b)** Configuration b of the antenna system, **(c)** Configuration *c* of the antenna system, **(d)** Input resistance and input reactance

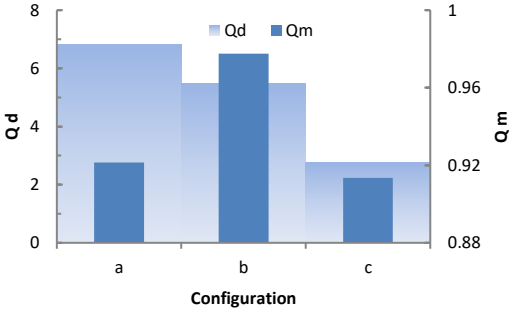

a

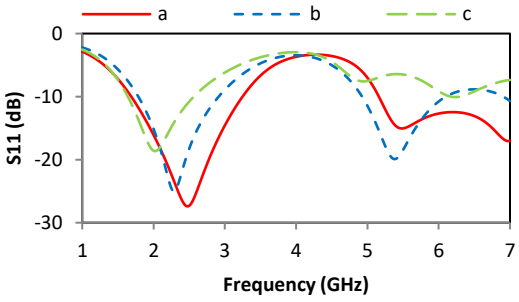

b

Fig. 9. *Quality factors and return losses for each configuration*
(a) The quality factors of the two modes for the configurations *a*, *b* and *c*, **(b)** Return loss of the antenna system for the three configurations red (solid) line =configuration *a*, blue (dashed) line =configuration *b* and green (dashed) line =configuration *c*.

Table 1 Elements values for different configurations (DRA mode)

Configuration	N_{sm}	N_{md}	L_d	C_d	R_d
a	2.10	0.268	1 nH	0.5 pF	600 Ω
b	2.16	0.242	1 nH	0.5 pF	600 Ω
c	3.21	0.152	1 nH	0.5 pF	600 Ω

The return losses for each of the configurations are shown in Fig. 9(b). It is evident that for configuration *a* and *b* the desired mode of the dielectric resonator is coupled to the source. It can also be seen from Fig. 9(b) that the DR is not coupled to the source for configuration *c*.

Fig. 10(a) shows the input impedance of the hybrid antenna system, the proposed model (Fig. 6(b)) approximates the optimized antenna accurately with elements values given in Table 2.

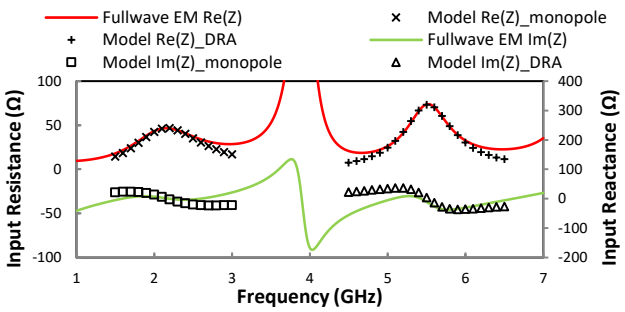

a

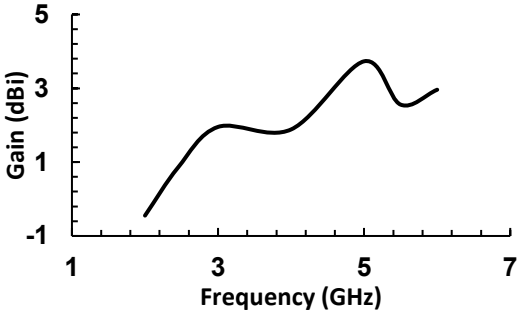

b

Fig. 10. *Input impedance and gain of the hybrid antenna system*
(a) The input impedance of the hybrid antenna system, **(b)** Gain of the antenna

Table 2 Elements values for the hybrid antenna system

Parameter	*Monopole mode*	*DRA mode*
N_{sm}	1.35	2.15
N_{md}	10	0.268
R_m	27 Ω	27 Ω
L_m	1 nH	1 nH
C_m	5.44 pF	5.44 pF
R_d	600 Ω	600 Ω
L_d	1 nH	1 nH
C_d	0.5 pF	0.5 pF

The gain of the antenna is shown in Fig. 10(b). The efficiency of the antenna for the monopole mode is 95% and for the DRA mode is 96%.

4. Results and Discussion

The combined DRA-Monopole antenna structure has been optimized and developed (Fig. 11). The dielectric resonator having ε_r of 9.5 and dimensions, d = 18mm and h = 6mm is attached to the PCB with a conducting glue. The PCB material chosen here is Rogers RT5880 having ε_r = 2.2 and substrate height of 1.575 mm. The simulated and measured return loss of the dual-band hybrid antenna system is illustrated in Fig. 11. As it can be seen from Fig. 11 the measured lower frequency band is moved from the desired frequency band, this was due to the imperfection in the fabrication of prototype. Nevertheless the dual-band phenomena can well be studied with this structure.

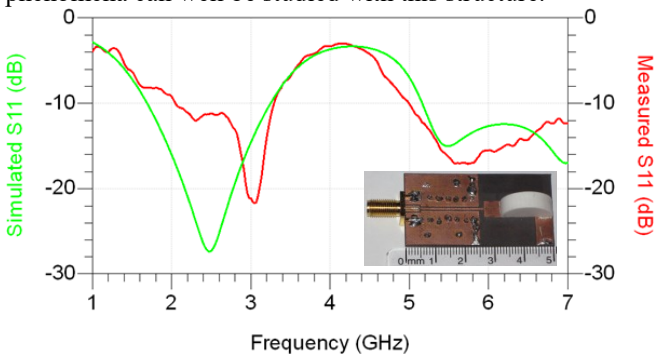

Fig. 11. *Simulated and measured return loss of the proposed filter. Structure of the fabricated filter (bottom right inset).*

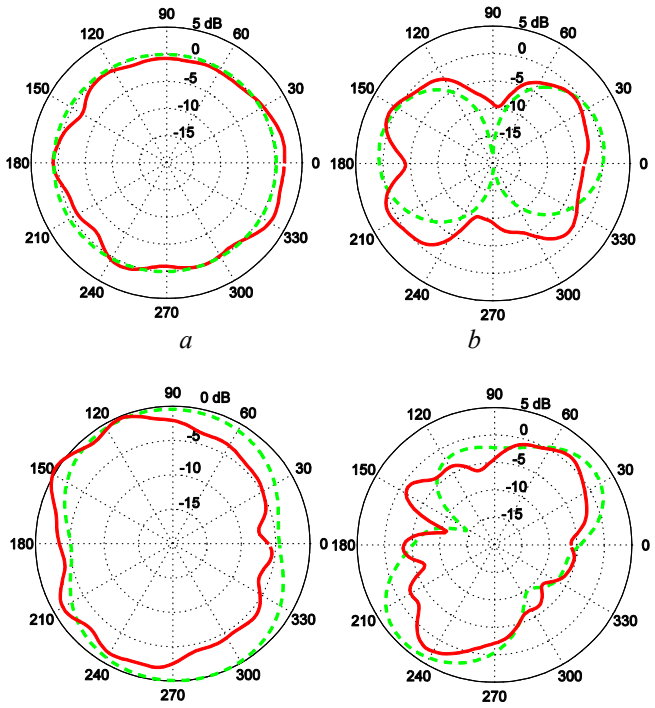

a *b* *c* *d*

Fig. 12. *Radiation patterns (Gain vs θ). Simulated values in dashed green lines and measured values in solid red line.*
(a) ϕ= 0° (x-z plane) at f_L, **(b)** ϕ= 90° (y-z plane) at f_L, **(c)** ϕ= 0° (x-z plane) at f_U, **(d)** ϕ= 90° (y-z plane) at f_U

The simulated and the measured radiation patterns, as shown in Figs. 12(a) and (b), at the lower frequency band f_L the results show good similarity although 3-5 dB loss is observed (for ϕ= 0°) in the measurement results. A little deterioration is observed in the radiation pattern at θ= 180°– back side of the DR (for ϕ= 90°). At the upper frequency band centred at f_U the radiation patterns of the simulation and the measurements can be compared from Figs. 12(c) and (d). The patterns for the band at f_U can be compared with that of Fig. 3. The patterns are quite similar except where the effect due to finite ground plane is dominant, which is more clear in the plot of ϕ= 0° plane. Comparing Fig. 3(a) and Fig. 12(c) it can be observed that the two nulls appearing in Fig. 3(a) at θ=90° and θ=270° cannot be seen in

Fig. 12(c) as there is significant loss of ground plane at $\phi = 0^o$ plane of the final structure (Fig. 11).

The proposed methodology can be employed to design any antenna system, for example, monopole can be replaced by a patch antenna, and the same principle could be followed to extract the model parameters. In that case, the desired patch antenna mode will be characterized for coupling with the DRA mode as well as with the source. Similarly, the DRA will be analysed for its dependence on the patch antenna mode, which will then be coupled to the source. Once all the model parameters are known, the complete antenna system can easily be designed. Furthermore, this methodology can be extended to multiple radiating modes (more than two) that may couple to each other in complex coupling topologies. The model derived from the above procedure can be used to integrate with other front-end components or co-designing of subsystems exhibiting multiple functionalities such as filter-antenna or antenna-amplifier subsystems. The design process is systematically summarized below:

Step 1. Characterize the elements starting with the element having less couplings and moving towards those with more couplings.

Step 2. Analyse the results and find the variables and structure to achieve quasi-independent design of each radiating mode.

Step 3. Extract the model parameters for each radiating mode based on the analyses from the previous step.

Step 4. Optimize the combined system. The generated model can now be used, reliably, to optimize the whole multiband radiating system.

Step 5. Integrate the optimized model with the rest of front-end components. The generated model can now easily be integrated with other circuit elements, which consequently simplifies the hybrid (EM + circuit) system design process.

5. Conclusion

A detailed designed methodology for dual-band antennas has been proposed. The proposed methodology is employed for designing a dual-band hybrid DRA-Monopole antenna. Since the hybrid antenna consists of two inter-dependent radiating elements, a comprehensive coupling analysis has been presented. A reliable circuit model has been proposed which caters for the off-resonance loading effect on both the modes (monopole antenna mode and the DRA mode). It has been demonstrated that the two hybrid radiating modes can be designed quasi-independently. The proposed design methodology simplifies the design procedure for complex radiating systems.

6. References

[1] Lim, K., Pinel, S., Davis, M., Sutono, A., Lee, C. H., Heo, D., Obatoynbo, A., Laskar, J., Tantzeris, E., Tummala, R.: 'RF-system-on-package (SOP) for wireless communications', IEEE Microwave Magazine, 2002, **3,** (1), pp. 88-99

[2] Suga, R., Nakano, H., Hirachi, Y., Hirokawa, J., Ando, M.: 'Cost-Effective 60-GHz Antenna Package With End-Fire Radiation for Wireless File-Transfer System', IEEE Transactions on Microwave Theory and Techniques, 2010, **58**, (12), pp. 3989-3995

[3] Hong, W., Baek, K. H., Goudelev, A.: 'Multilayer Antenna Package for IEEE 802.11ad Employing Ultralow-Cost FR4', IEEE Transactions on Antennas and Propagation, 2012, **60**, (12), pp. 5932-5938

[4] Mun, B., Jung, C., Park, M. J., Lee, B.: 'A Compact Frequency-Reconfigurable Multiband LTE MIMO Antenna for Laptop Applications', IEEE Antennas and Wireless Propagation Letters, 2014, **13**, pp. 1389-1392

[5] Sung, Y.: 'Multi-band reconfigurable antenna for mobile handset applications', IET Microwaves, Antennas & Propagation, 2014, **8**, (11), pp. 864-871

[6] Ban, Y. L., Qiang, Y. F., Wu, G., Wang, H., Wong, K. L.: 'Reconfigurable narrow-frame antenna for LTE/WWAN metal-rimmed smartphone applications', IET Microwaves, Antennas & Propagation, 2016, **10**, (10), pp. 1092-1100

[7] Zheng, D. Z., Chu, Q. X.: 'A Multimode Wideband $\pm 45^o$ Dual-Polarized Antenna with Embedded Loops', IEEE Antennas and Wireless Propagation Letters, 2016, **PP**, (99), pp. 1-1

[8] Mao, C. X., Gao, S., Wang, Y., Qin, F., Chu, Q. X.: 'Multimode Resonator-Fed Dual-Polarized Antenna Array With Enhanced Bandwidth and Selectivity', IEEE Transactions on Antennas and Propagation, 2015, **63**, (12), pp. 5492-5499

[9] Zhang, Z., Shaoqiu, X., Li, Y., Wang, B. Z.: 'A Circularly Polarized Multimode Patch Antenna for the Generation of Multiple Orbital Angular Momentum Modes', IEEE Antennas and Wireless Propagation Letters, 2016, **PP**, (99), pp. 1-1

[10] Jan, J. Y.: 'Single-layer single-feed dual-frequency circular microstrip antenna with an offset open-ring slot', IEEE Transactions on Antennas and Propagation, 2003, **51**, (10), pp. 3010-3012

[11] Chen, S., Liu, G., Chen, X., Lin, T., Liu, X. Duan, Z.: 'Compact Dual-Band GPS Microstrip Antenna Using Multilayer LTCC Substrate', IEEE Antennas and Wireless Propagation Letters, 2010, **9,** pp. 421-423

[12] Antoniades, M. A., Dadgarpour, A., Razali, A. R., Abbosh, A., Denidni, T. A.: 'Planar antennas for compact multiband transceivers using a microstrip feedline and multiple open-ended ground slots', IET Microwaves, Antennas & Propagation, 2015, **9**, (5), pp. 486-494

[13] Guan, D. F., Qian, Z. P., Cao, W. Q., Ji, L. Y., Zhang, Y. S.: 'Compact SIW Annular Ring Slot Antenna With Multiband Multimode Characteristics', IEEE Transactions on Antennas and Propagation, 2015, **63**, (12), pp. 5918-5922

[14] Fang, X., Leung, K. W., Lim, E. H.: 'Singly-Fed Dual-Band Circularly Polarized Dielectric Resonator Antenna', IEEE Antennas and Wireless Propagation Letters, 2014, **13**, pp. 995-998

[15] Rao, Q., Denidni, T., Sebak, A.: 'A hybrid resonator antenna suitable for wireless communication applications at 1.9 and 2.45 GHz', IEEE Antennas and Wireless Propagation Letters, 2005, **4**, pp. 341-343

[16] Okano, Y., Takatsuka, M., Mizutani, T., Fujisawa, S.: 'Novel Hybrid Antenna for Broadcasting Satellite and Terrestrial HD-TV', IEEE Transactions on Antennas and Propagation, 2015, **63**, (4), pp. 1425-1435

[17] Pan, G., Li, Y., Zhang, Z., Feng, Z.: 'A Compact Wideband Slot-Loop Hybrid Antenna with a Monopole Feed', IEEE Transactions on Antennas and Propagation, 2014, **62**, (7), pp. 3864-3868
[18] Wu, R., Chu, Q. X.: 'Resonator-loaded Broadband Antenna for LTE700/GSM850/GSM900 Base Stations', IEEE Antennas Wireless Propagation Letters, 2016, **PP**, (99), pp.1-1
[19] Guha, D., Antar, Y. M. M., Ittipiboon, A., Petosa, A., Lee, d.: 'Improved Design Guidelines for the Ultra Wideband Monopole-Dielectric Resonator Antenna', IEEE Antennas and Wireless Propagation Letters, December 2006, **5**, (1), pp. 373-376
[20] Naeem, U., Bila, S., Verdeyme, S., Chreim, H., Chantalat, R., Thévenot, M., Monediere, T., Palacin, B., Cailloce, Y.: 'A simplified methodology for matched filter design with constraints — filter–antenna subsystem for space application'. IEEE MTT-S Int. Microwave Symp. Digest, Anaheim, CA, USA, 23-28 May 2010, pp. 1664–1667
[21] Naeem, U., Bila, S., Verdeyme, S., Thevenot, M., Monediere, T.: 'A compact dual band filter-antenna subsystem for 802.11 Wi-Fi applications'. European Wireless Technology Conference (EuWIT), Paris, France, 27-28 September 2010, pp. 181-184
[22] Petosa, A., Ittipiboon, A., Antar, Y., Roscoe, D., Cuhaci, M.: 'Recent advances in dielectric-resonator antenna technology', IEEE Antennas and Propagation Magazine, 1998, **40**, pp. 35-48
[23] Long, S.A., McAllister, M., Liang Shen: 'The resonant cylindrical dielectric cavity antenna', IEEE Transactions on Antennas and Propagation, 1983, **31**, (3), pp. 406-412